



### **Science Arts & Métiers (SAM)**

is an open access repository that collects the work of Arts et Métiers Institute of Technology researchers and makes it freely available over the web where possible.

This is an author-deposited version published in: <https://sam.ensam.eu>  
Handle ID: <http://hdl.handle.net/10985/23306>

#### **To cite this version :**

Guillaume MARTIN, Etienne BALMES, Thierry CHANCELIER, Sylvain THOUVIOT, Rémi LEMAIRE - A Structural Dynamics Modification Strategy based on Expanded Squeal Operational Deflection Shapes - In: Eurobrake, Allemagne, 2022-05-17 - Eurobrake 2022 : - 2022

Any correspondence concerning this service should be sent to the repository

Administrator : [scienceouverte@ensam.eu](mailto:scienceouverte@ensam.eu)



# A Structural Dynamics Modification Strategy based on Expanded Squeal Operational Deflection Shapes

\*Guillaume Martin<sup>1</sup>, Etienne Balmes<sup>1,2</sup>, Thierry Chancelier<sup>3</sup>, Sylvain Thouviot<sup>3</sup>, Rémi Lemaire<sup>3</sup>

<sup>1</sup>SDTools

44 Rue Vergniaud, 75013 Paris, France (E-mail: [martin;balmes]@mail.sdtools.com)

<sup>2</sup>Processes and Engineering in Mechanics and Materials laboratory (PIMM) ENSAM, CNRS, CNAM, HESAM Université  
151 Boulevard de l'Hôpital, 75013 Paris, France (E-mail: balmes@ensam.eu)

<sup>3</sup>Hitachi Astemo France S.A.S.

126 rue de Stalingrad, 93700 Drancy, France (E-mail: [thierry.chancelier;sylvain.thouviot;remi.lemaire]@hitachiastemo.com)

DOI (FISITA USE ONLY)

**ABSTRACT:** To analyze brake squeal, measurements are performed to extract Operational Deflection Shapes (ODS) characteristic of the limit cycle. The advantage of this strategy is that the real system behavior is captured, but measurements suffer from a low spatial distribution and hidden surfaces, so that interpretation is sometimes difficult. It is even more difficult to propose system modifications from test alone. Historical Structural Dynamics Modification (SDM) techniques need mass normalized shapes which is not available from an ODS measurement. Furthermore, it is very difficult to translate mass, damping or stiffness modification between sensors into physical modifications of the real system. On the model side, FEM methodology gives access to fine geometric details, continuous field over the whole system. Simple simulation of the impact of modifications is possible, one typical strategy for squeal being to avoid unstable poles. Nevertheless, to ensure accurate predictions, test/FEM correlation must be checked and model updating may be necessary despite high cost and absence of guarantee on results. To combine both strategies, expansion techniques seek to estimate the ODS on all FEM DOF using a multi-objective optimization combining test and model errors. The high number of sensors compensates for modeling errors, while allowing imperfect test. The Minimum Dynamics Residual Expansion (MDRE) method used here, ensures that the complex ODS expanded shapes are close enough to the measured motion but have smooth, physically representative, stress field, which is mandatory for further analysis. From the expanded ODS and using the model, the two underlying real shapes are mass-orthonormalized and stiffness-orthogonalized resulting in a reduced modal model with two modes defined at all model DOFs. Sensitivity analysis is then possible and the impact of thickness modifications on frequencies is estimated. This provides a novel structural modification strategy where the parameters are thickness distributions and the objective is to separate the frequencies associated with the two shapes found by expansion of the experimental ODS.

The methodology will be illustrated for a recent disk brake test and model.

**KEY WORDS:** Structural Dynamics Modifications, Operational Deflection Shapes, Minimum Dynamic Residual Expansion, Sensitivity analysis, Squeal

## 1. INTRODUCTION

To analyze brake squeal, measurements are performed to extract two Operational Deflection Shape (ODS) characteristic of the limit cycle. These shapes have the advantage to capture the real system behavior but suffer from low spatial distribution of sensors. Historical Structural Dynamics Modification (SDM) techniques allow to work directly on test data need but scaled modes are needed, which is not available from an ODS. Moreover, classical SDM strategies consider modifications that are point masses or relative springs/dampers between sensors that are very difficult to translate into physical modifications of the real system.

On the model side, the Finite Element Method (FEM) gives access to fine geometric details, continuous field over the whole system. Simple simulation of the impact of modifications is possible, one typical strategy for squeal handling being to separate modal frequencies to avoid interactions involved in squeal. However, to

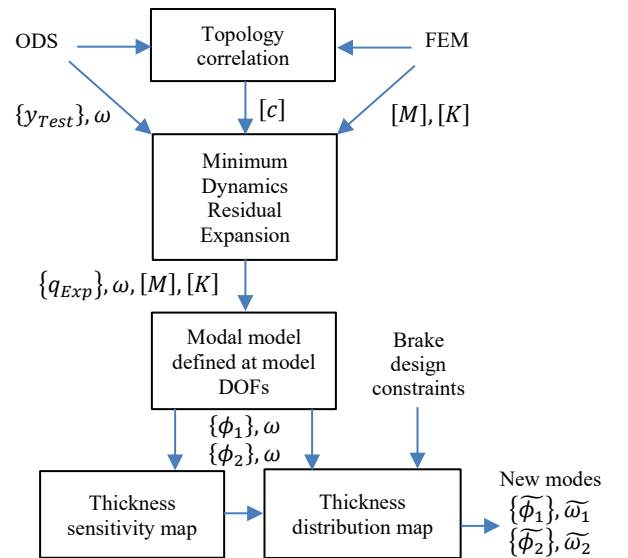


Figure 1 SDM after expansion procedure

ensure accurate predictions, test/FEM correlation must be checked and model updating may be necessary despite high cost and absence of guarantee on results.

To combine the fine spatial description of FEM with the ability to work directly on test data provided by standard SDM strategies, the procedure summarized in **Erreur ! Source du renvoi introuvable.** has been developed. It relies on three main steps:

- expand ODS (defined at sensors) to estimate shapes at all model DOFs using the Minimum Dynamics Residual Expansion (MDRE)
- build an approximate modal model with the ODS shapes at the limit cycle frequency
- use a novel SDM strategy, where the parameters are thickness distributions on the model surface, to predict mode frequency evolutions

Section 2 first presents the test case used as illustration throughout this paper: test geometry, measured ODS, FEM and topology correlation (model observation through sensors). ODS expansion and modal model estimation is then explained in section 3. Section 4 details the new SDM strategy and a consistency check is performed. The full procedure is finally applied in section 5 to the test case: a thickness distribution map is proposed that should reduce the squeal occurrence.

## 2. TEST CASE DESCRIPTION

The test case used is a Hitachi Astemo disc brake presenting a squeal occurrence near 4050Hz. To understand the behavior, an ODS measurement is performed using a 3D Scanning Laser Doppler Vibrometer (3D-SLDV). The test wireframe composed of 1293 sensors (431 points) is superposed over the FEM in Figure 2. Individual sensors are represented as red arrows on figure left. The gap between each wireframe node and the closest model surface is shown on figure right to evaluate the topology correlation.

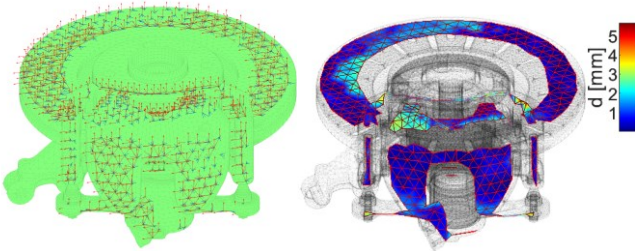


Figure 2 Test case topology correlation: sensors as red arrows (left) and node to surface distance map (right)

Squeal is reproduced on a dyno test bench with constant brake pressure and constant disc rotational speed. When squeal occurs, the 3D-SLDV sequentially scans all points. Using reference accelerometers placed on the brake system, the sequential measurements are then combined using the procedure developed in [1] which deals with the variation of the limit cycle in frequency, amplitude and shape due to the wheel spin. A complex shape is obtained, which contains the two main real shapes that interact throughout the limit cycle. This complex shape is shown in Figure

5 left, highlighting a classical lobe motion of the disc and a deformation localized at the center and right part of the bracket.

On the model side, a non-linear static analysis is first performed to obtain the contact stiffness distributions engendered by braking pressure and torque. The model is linearized around this static state, and a Complex Eigenvalue Analysis is performed [2]. The correlation between complex mode shapes and the ODS is evaluated using the Modal Assurance Criterion [3]. At this stage, the best scenario is when there is good agreement between one numerical mode close to the squeal frequency and the ODS. The model is thus deemed representative and used with confidence to propose squeal countermeasures.

Often, the correlation is not satisfying, which comes either from test, model or both. The model may not be representative enough of the true system dynamics. The test may lead to a limit cycle where non-linearities are high enough to modify shapes notably from a combination of two nearby modes that are the classical origin of instabilities [4], [5]. Other test error sources such as noise, bad sensor location,... can also contribute the low correlation [6].

For this case, with no satisfying correlation between test and analysis, the MDRE method presented in the next section gives a appropriate methodology to estimate the model response from measurement and a not fully wrong model.

## 3. EXPANSION AND MODAL MODEL

One difficulty with vibration measurements is the low spatial resolution. Even for 3D-SLDV sensors, motion of hidden or unreachable parts cannot be measured. The first objective of expansion methods is the estimation of the motion at all DOFs of a model from an experimental shape defined at sensors. Several expansion methods have been developed such as static [7], dynamic [8], Error in Constitutive Relation [9] and MDRE [10]. The two last methods introduce the idea that both modeling and test errors can be defined and combined into a multi-objective cost function.

Section 3.1 quickly reminds the MDRE theory. It is applied to the test case in section 3.2 with a fine tuning of the balance between modeling and test error to ensure that the expanded ODS is close enough to the measured motion but has smooth stress field. This is mandatory to obtain a physically representative modal model in section 3.3 on which the proposed novel SDM strategy can be applied.

### 3.1. Theory of Minimum Dynamic Residual Expansion

MDRE combines a modeling error  $\epsilon_{Mod}$  and a test error  $\epsilon_{Test}$ . The two errors depend on the expanded shape  $\{q_{Exp}\}$  defined at all model DOF which corresponds to the shape minimizing the multi-objective cost function

$$J(\{q_{Exp}\}, \gamma) = \epsilon_{Mod}(\{q_{Exp}\}) + \gamma \epsilon_{Test}(\{q_{Exp}\}) \quad (1)$$

where the weighting coefficient  $\gamma$  leads to verification of model equations for low values and exact observation of the test for high values.

To measure the difference between the expanded shape  $\{q_{Exp}\}$  and the test measurement  $\{y_{Test}\}$ , the model is first observed at sensors using an observation matrix  $[c]_{NS \times NDOF}$  built from the test/FEM superposition. The test error is then defined by

$$\epsilon_{Test}(q_{Exp}) = \|\{y_{Test}\} - [c]\{q_{Exp}\}\|^2 \quad (2)$$

To evaluate how the model is forced to follow the test, dynamic residual loads  $\{R_L\}$  and the associated energy norm  $K$  define the modeling error

$$\epsilon_{Mod}(q_{Exp}) = \|\{R_L\}\|_K^2 = \|([K] - \omega^2[M])\{q_{Exp}\}\|_K^2 \quad (3)$$

with  $[K]$ ,  $[M]$ , the stiffness and mass matrices and  $\omega$  the expansion pulsation. One notes that  $\{R_L\} = 0$  is equivalent to say that  $\{q_{Exp}\}$  is a normal mode and  $\omega$  the associated modal frequency.

More details on the implementation, norm definitions and examples can be found in [1], [11]. One just reminds here that model reduction is mandatory to solve the expansion in an acceptable time. This reduction is performed on the basis composed by the normal mode shapes  $\{\phi\}_M$  and the enrichment with static loads at sensors  $[T_{Sens}^\perp]$ . The reduced coordinates can thus be split in two

$$\{q\} = [T]\{q_R\} = [\phi_M \quad T_{Sens}^\perp] \begin{Bmatrix} q_M \\ q_\perp \end{Bmatrix} \quad (4)$$

with  $q_M$  the part linked to the model modes and  $q_\perp$  the part linked to the enrichment at sensors.

The test case used has 1.7 million model DOFs and 1293 vibrometer sensors. The offline phase consisting in computing 100 normal modes and the enrichment with 1293 static loads at sensors takes about an hour. Computing the expanded shape associated to a single  $\gamma$  only takes a second.

### 3.2. Expansion result

The ODS shown in Figure 5 left is expanded using MDRE for several values of the  $\gamma$  weight equally spaced on a logarithmic scale. Increasing  $\gamma$  gives more and more weight to the test error on the multi-objective cost function (1): the test error decreases up to 0 while the modeling increases to its maximum. To display modeling and test error evolution whose values are not in the same range, the relative error is defined

$$\epsilon_{Test}^R = \frac{\epsilon_{Test}}{\|y_{Test}\|} ; \epsilon_{Mod}^R = \frac{\epsilon_{Mod}}{\|q_{Exp}\|_K} \quad (5)$$

and the relative model error is split in a part linked to the normal modes and a part linked to the sensor enrichment using (4).

Figure 3 shows the evolution of the relative test and modeling errors with  $\gamma$ . An interesting value is found at  $\gamma = 1e4$ . For lower values, modeling error was mainly due to the modal part. Higher  $\gamma$  values lead to a quick increase of the modeling error due to the enrichment part, which can occur because noise is transferred from the test error to the modeling error or because dynamics are missing in the normal mode part to better match the measurement.

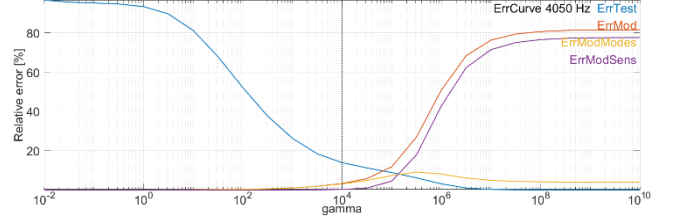


Figure 3 Evolution with  $\gamma$  of relative test and modeling errors

Display of the spatial repartition of modeling and test errors is helpful to go deeper in the analysis of sources of bad correlation as can be seen in [1], [11], [12] which is helpful if model updating must be performed. This is not the main topic for this paper so it will not be developed here. Authors want to mention that figures similar to Figure 3 were wrong in previous papers [9], [10], model errors linked to mode and enrichment parts being inverted: this is corrected here with a more convincing interpretation.

The choice of  $\gamma$  has a high influence on the stress field of the expanded shape. In Figure 4 right, a too high value of  $\gamma$  leads to stress concentration at sensors which is clearly not physical and thus cannot be used for further model error localization or sensitivity studies.

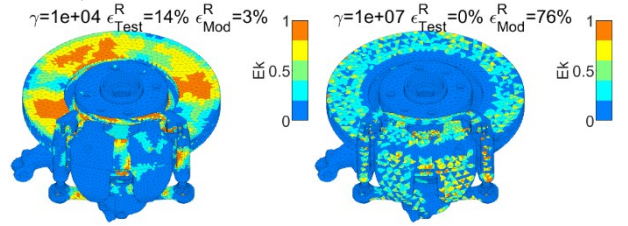


Figure 4 Stress field of expanded shape for  $\gamma = 1e4$  (left) and  $\gamma = 1e7$  (right)

$\gamma = 1e4$  is thus finally chosen and is quite satisfying: the relative test error of 15% is reasonable since the test shape contains noise and the relative modeling error is very low at about 5%. This answers the question raised at the end of section 2: despite the absence of correlation between mode shapes and ODS, relatively small residual loads are needed to reproduce the ODS so that the model accuracy is acceptable. Figure 5 shows the measured ODS on the left and the retained expanded shape on the right.



Figure 5 Squeal ODS (left) and expanded shape with  $\gamma = 1e4$  (right)

When the modeling error is too high, model updating is necessary to gain confidence in the prediction of system evolution in response to modifications. Even if model updating is always useful, it often takes long time and there is no guarantee to reach satisfying results. In the meantime, the expansion gives access to a shape defined at all model DOFs with good agreement with the real system. This



can be exploited to build a simple modal model on which SDM can be applied.

### 3.3. Modal model from ODS expansion

To perform SDM, a modal model is needed. Standard modal scaling uses collocated measurements (input load and output motion at the same location and direction) which is not available for ODS because the system excitation is neither controlled nor measured. To still obtain a modal model, the real and imaginary parts of the complex expanded ODS are extracted and the two are mass-orthonormalized and stiffness-orthogonalized with the nominal model. This leads to reduced mass matrix, stiffness matrix and basis

$$[M_R] = \begin{bmatrix} 1 & 0 \\ 0 & 1 \end{bmatrix}; [K_R] = \begin{bmatrix} \omega_1^2 & 0 \\ 0 & \omega_2^2 \end{bmatrix}; [T] = [\phi_1 \phi_2] \quad (6)$$

Figure 6 shows these two shapes for the illustrated application. Because these are obtained from expansion allowing modeling error, the two corresponding frequencies  $f_1 = \omega_1/2\pi$  and  $f_2 = \omega_2/2\pi$  are higher than the expansion frequency (4050Hz): the first shape is at 4119Hz ( $\Delta f/f = 1.7\%$ ) and the second at 4217Hz ( $\Delta f/f = 4.1\%$ ).

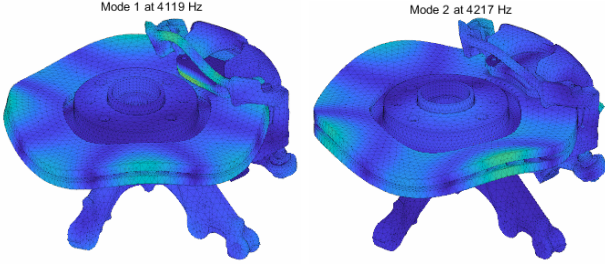


Figure 6 Modal model shapes built from ODS expansion

To correct these frequency shifts, diagonal values of the reduced stiffness matrix are modified to correspond to the expected limit cycle frequency. Reduced matrices actually used for further SDM are thus

$$[M_R] = \begin{bmatrix} 1 & 0 \\ 0 & 1 \end{bmatrix}; [K_R] = \begin{bmatrix} \omega^2 & 0 \\ 0 & \omega^2 \end{bmatrix}; [T] = [\phi_1 \phi_2] \quad (7)$$

with  $\omega = 2\pi * 4050 \text{ rad/s}$

## 4. STRUCTURAL DYNAMICS MODIFICATION

From a modal model, SDM techniques allow to predict the evolution of modes in response to modifications. SDM theory in section 4.1 and limitations of the historical use of SDM lead to the proposition of a new strategy in section 4.2 which relies on sensitivity analysis to thickness modifications. Consistency is finally checked in section 4.3.

### 4.1. SDM theory

The objective of SDM is to estimate the influence of a structural modification (typically modification of mass and stiffness) from a second order reduced modal model

$$(-\omega^2[M_R] + [K_R])\{q_R\} = 0 \quad (8)$$

with  $[M_R] = [T]^T[M][T]$ ;  $[K_R] = [T]^T[K][T]$  and  $[T]$  the reduction basis defined at specific output locations.

Even without a full knowledge of  $[M]$ , it is possible to introduce modifications of

- mass  $[\Delta M]$  at output locations

- stiffness  $[\Delta K]$  between outputs

With the hypothesis that the reduced basis subspace remains representative enough, these modifications are projected on this basis and introduced in the model

$$(-\omega^2([M_R] + [\Delta M_R]) + ([K_R] + [\Delta K_R]))\{q_R\} = 0 \quad (9)$$

with  $[\Delta M_R] = [T]^T[\Delta M][T]$  and  $[\Delta K_R] = [T]^T[\Delta K][T]$

New modes associated to this modified reduced model allow to evaluate frequency shifts and eventually shape evolution (combination of reduced basis vectors).

Historically [13], [14], the modal model is built from experimental modal analysis with the basis  $[T]$  being composed of identified mode shapes defined at sensors. These modes are normalized using colocalized transfers so that  $[M_R] = [I]$  and  $[K_R] = [\omega^2]$  the diagonal matrix of squared mode pulsations. The main drawback of this strategy is that model outputs are sensors and thus mass and stiffness modifications are only possible at sensor locations: add/remove mass at sensor locations or add/remove stiffness between sensors. It is then very difficult to interpret these very coarse modifications as real physical modifications of the real system.

To allow more realistic modifications, the use of expansion technique was proposed in [15]: the reduction basis  $[T]$  is extended from outputs at sensors to outputs at all model DOFs. An example shown in Figure 7 left highlights that after expansion it is possible to connect a stiffener whereas interface nodes do not correspond to measured points. After expansion, we have a direct access to the mass and stiffness assembly matrices corresponding to each element: mass  $[\Delta M]$  and stiffness  $[\Delta K]$  modifications in equation (9) corresponding to the removal of some elements is easily tested.

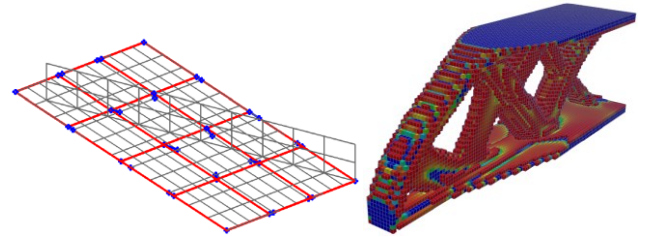


Figure 7 Modification adding stiffener [15] and topology optimization example [16]

Another objective is to obtain realistic modifications. For this purpose, the first thought would be addition/removal of elements as in topology optimization techniques [16] illustrated in Figure 7 right. While quite precise spatially, this strategy still ends up with a rather coarse description of the final surface and is limited to element removal only. A new SDM strategy that tackles both issues is thus proposed in the next section.

#### 4.2. A SDM using thickness modification

The proposed SDM strategy is based on the sensitivity analysis of the reduced model modal frequencies to thickness modification at the component surfaces. Without entering into the details which can be found in [17], the sensitivity of a modal frequency to a parameter  $p$  is related the sensitivity of the mass and stiffness matrices to this parameter  $p$  projected on the mode

$$\frac{\partial \omega_j^2}{\partial p} = \{\phi_j\}^T \left( \frac{\partial K}{\partial p} - \omega_j^2 \frac{\partial M}{\partial p} \right) \{\phi_j\} \quad (10)$$

with  $\omega_j$  and  $\{\phi_j\}$  the pulsation and shape of mode  $j$ .

Rearrangement of this equation gives an energy interpretation: the evolution of the squared modal frequency is equal to twice the difference between the strain and kinetic energy evolution.

$$\frac{\partial \omega_j^2}{\partial p} = \{\phi_j\}^T \frac{\partial K}{\partial p} \{\phi_j\} - \{\phi_j\}^T \omega_j^2 \frac{\partial M}{\partial p} \{\phi_j\} = 2 * \left( \frac{\partial E_{k,l}}{\partial p} - \frac{\partial E_{m,l}}{\partial p} \right) \quad (11)$$

The parameter  $p$  for this study is a small thickness increase at the component surfaces. A thin layer of finite elements is built by extruding the external surface of the structure in the normal direction. This is illustrated with the test case in which thickness modifications are evaluated for the caliper and bracket components shown on Figure 8 left. The map of normals to the external surface shown on top right is used to extrude the thin layer shown at bottom right (thickness is increased to 1mm on the image for visualization purpose, but the actual thickness for computation is 0.01mm)

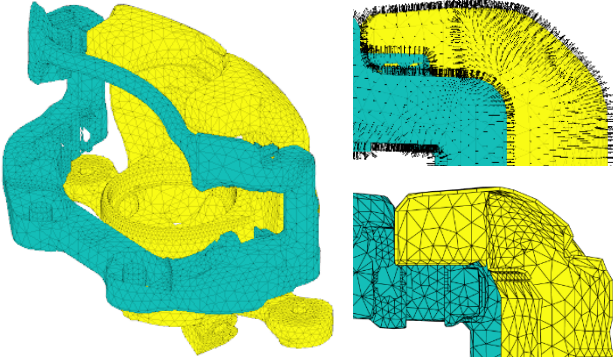


Figure 8 Caliper yellow and bracket green component (left), normal map (top right) and thin layer (bottom right)

On this thin layer, motion is only known at the initial surface (set of nodes  $a$ ). To estimate the motion of extruded nodes (set of nodes  $b$ ), dynamic expansion is performed. Motion known at DOFs  $\{q_a\}$  is enforced and motion sought at DOFs  $\{q_b\}$  is computed by allowing external forces  $\{F_a\}$  at known DOFs only

$$\begin{bmatrix} Z_{aa}(\omega) & Z_{ab}(\omega) \\ Z_{ba}(\omega) & Z_{bb}(\omega) \end{bmatrix} \begin{Bmatrix} q_a(\omega) \\ q_b(\omega) \end{Bmatrix} = \begin{Bmatrix} F_a(\omega) \\ 0 \end{Bmatrix} \quad (12)$$

$$\begin{Bmatrix} q_a(\omega) \\ q_b(\omega) \end{Bmatrix} = \begin{bmatrix} I \\ Z_{bb}^{-1}(\omega) Z_{ba}(\omega) \end{bmatrix} \{q_a(\omega)\} \quad (13)$$

with  $Z(\omega) = (-\omega^2 M + K)$  the dynamic stiffness

As illustration, Figure 9 shows the estimated motion of the thin layer for a mode of interest.

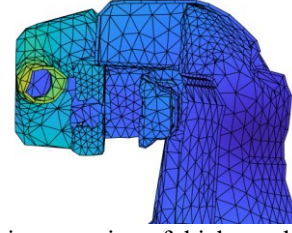


Figure 9 Dynamic expansion of thickness layer

Strain and kinetic energy are then computed at Gauss points of the thickness layer and energy density maps on the surface are obtained as shown in Figure 10. The difference between strain and kinetic energy density maps gives the thickness sensitivity map (or “shift” energy density map): it is directly related to the frequency shift from the sensitivity equation (11).

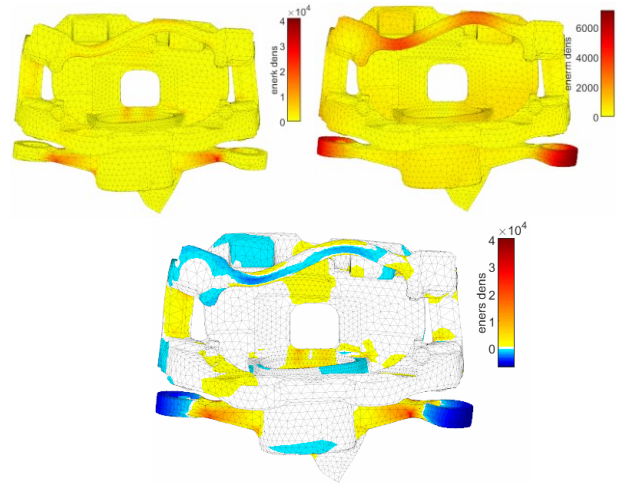


Figure 10 Energy density maps: strain energy (top left), kinetic energy (top right) and shift energy (bottom)

In areas with positive shift energy density, thickness increase adds more strain energy than kinetic energy thus increasing the modal frequency. To also increase the modal frequency in areas with negative shift energy, the extrusion should be in a negative direction corresponding to removing material.

From the thickness sensitivity map, a thickness distribution map is derived. Note that this step is generally not straightforward as many constraints must be respected such as

- Do not deform functional surfaces
- Avoid removing too much material to ensure brake performances and durability
- Avoid adding too much material to limit material costs and brake weight
- Keep smooth surface curvature
- ...

For the sake of simplicity, these difficulties are not addressed in this paper. The thickness distribution map is simply the thickness sensitivity map with maximum amplitude normalized to one, thus leading to a maximum thickness modification of 1mm. Because the thickness distribution map can be positive or negative, special attention must be paid to elements whose nodes are not all positively or negatively extruded. Figure 11 left shows three scenarii for each model element:

- Red element: all nodes are associated to a positive thickness value (material addition). Extrude outside the surface to get positive volume and count energy positively
- Blue element: all nodes are associated to a negative thickness value (material removal). Extrude inside the surface to get positive volume but count energy negatively
- Grey element: nodes are associated to positive and negative thickness values. The element volume is shrunk, thus not reliable and finally removed from the thickness layer. Nevertheless, it would have contained very low energy content (around zero thickness modification)

Figure 11 right shows the element kept in the layer. Like previously, dynamic expansion from known displacement at the nominal surface is performed to get the motion of the whole layer.

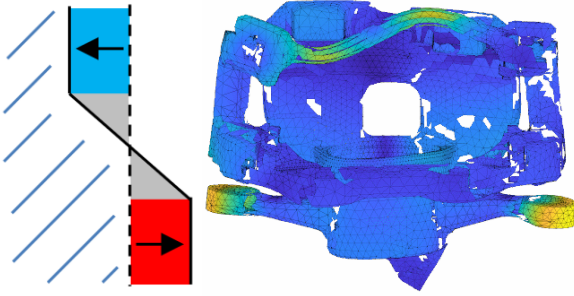


Figure 11 Extrusion direction and warped element (left), dynamic expansion on retained elements (right)

Using the equation (11), the evolution of the modal frequency in response to this modification is obtained from the nominal frequency  $\omega_{nom}$ , the strain energy  $\Delta E_k$  and the kinetic energy  $\Delta E_m$  contained in the thickness layer.

$$\omega_{new} = \sqrt{\omega_{nom}^2 + 2 * (\Delta E_k - \Delta E_m)} \quad (14)$$

This strategy which looks at the frequency evolution of one mode at a time will be called SDM-1Mode. If more than one mode is available in the reduction basis, it is more interesting to come back to the SDM equation (9) to take into account the impact of the modification on all modes at once.

The mesh is split in two parts

- one containing elements of the nominal model whose reduced mass  $[M_R]$  and stiffness  $[K_R]$  matrices are those of equation (7)
- another with new elements for the modification. Since new nodes are added, the response of  $[T]$  on those nodes is estimated by dynamic expansion and the  $[\Delta M]$  and  $[\Delta K]$  were defined in equation (9).

Solving equation (9) then gives new modes for which both frequency and shape may vary. This second strategy which looks at the evolution of all modes at once will be called SDM-AllModes.

Note that all these steps are quite fast. In our example, the thin layer is about 250.000 DOFs: from a thickness distribution, extrusion, dynamic expansion and new mode computation only take 15s.

### 4.3. Consistency analysis

To evaluate the proposed SDM strategy, a consistency analysis must be performed. Because further application will be done on the ODS at 4050Hz, the closest nominal model mode (at 4005Hz) is chosen and one seeks to increase its frequency.

The thickness sensitivity map of this mode is shown in Figure 10. This map is directly applied as signed thickness distribution map to build the thickness layer, whose motion after dynamic expansion was shown on Figure 11 right. SDM-1Mode and SDM-AllModes are finally computed to evaluate mode evolution.

To obtain a reference, the same signed thickness distribution map is applied to the model using a morphing strategy [18]: surface nodes are moved and volume interior nodes smoothly follow to keep good element quality. Computation of mode shapes on the full morphed models performed: these modes are the reference ones (hereafter called true model modes).

Figure 12 shows, for thickness variations up to 5 mm, the comparison between true mode frequencies (solid line), SDM-1Mode predictions (line with x crosses) and SDM-AllModes values (dashed line). For all modes in this frequency band, the two SDM strategies are quite accurate even if SDM-AllModes is always closer to the true model mode evolution.

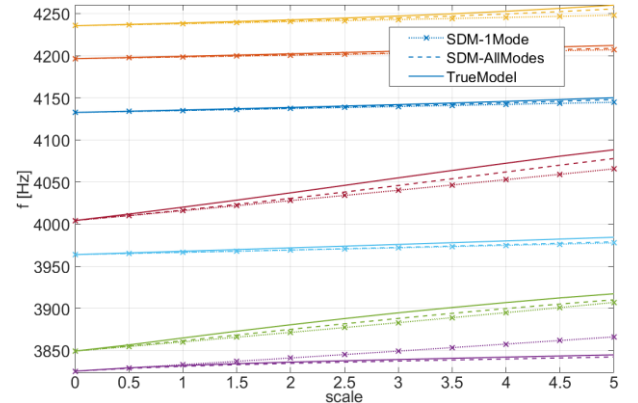


Figure 12 Comparison of SDM-1Mode and SDM-AllModes with true model frequency evolution in the frequency band of interest for the ODS

The major interest of using SDM-AllModes is found when close modes interact with each other. This is shown in Figure 13 where two modes cross around frequency 5575Hz and scale 2.5. SDM-AllModes is still very close to the true model evolution, but SDM-1Mode clearly fails in predicting the modal frequency evolution because shape evolution is not possible.



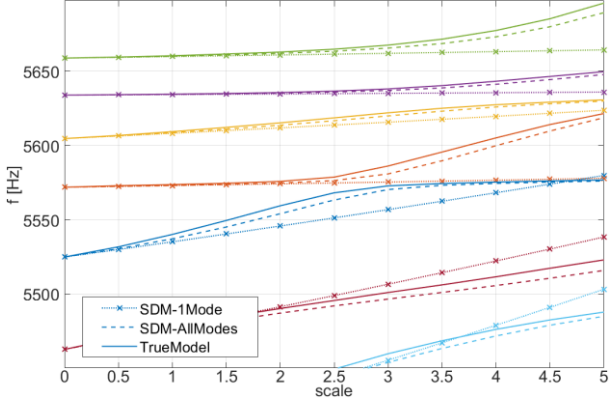


Figure 13 Comparison of SDM-1Mode and SDM-AllModes with true model frequency evolution in a frequency band where mode crossing occurs

## 5. SQUEAL REDUCTION OBJECTIVE: SEPARATE MODE FREQUENCIES

The final objective is to modify the system in order to reduce squeal occurrences. As explained in [12], brake instability can be analyzed as the interaction of real mode shapes (often mainly two) leading to a complex mode with negative damping. Making the hypothesis that the ODS complex shape contains the two main real shapes responsible of the instability, the idea is to separate them in frequency.

The SDM strategy detailed in section 4.2 is thus applied on the modal model obtained after expansion of the ODS in section 3.3. Figure 14 shows that for the first mode, areas with the highest thickness sensitivity are located on the top and left of the bracket and on top of the caliper. For the second mode, most sensitive areas are mainly on top of the caliper cylinder.

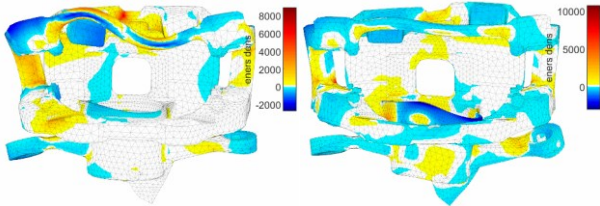


Figure 14 Thickness sensitivity map for the two modes of the modal model after ODS expansion

The objective being to separate frequencies, the map shown in Figure 15 is the difference between the two previous ones. In red areas, the gap between the first and the second mode frequencies increases whereas it is the contrary in blue areas.

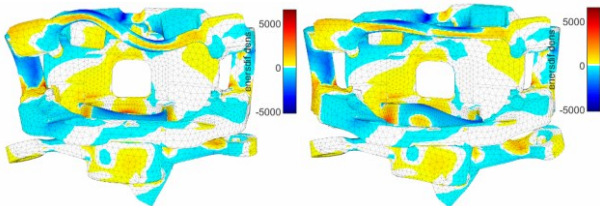


Figure 15 Sensitivity map to separate the frequencies displayed on the two mode shapes

One difficulty with this thickness sensitivity map is that few nodes have a very high value that would lead to very localized thickness increase. To smooth the map, it is first normalized with the maximum value set to one and then square root is applied to the values, reducing the gap between high and medium values. The resulting map is the thickness distribution finally applied with several scales going from -5 to 5 mm.

Figure 16 shows the evolution of the frequency in response to the thickness distribution maps. Both SDM-1Mode and SDM-AllModes give very close predictions.

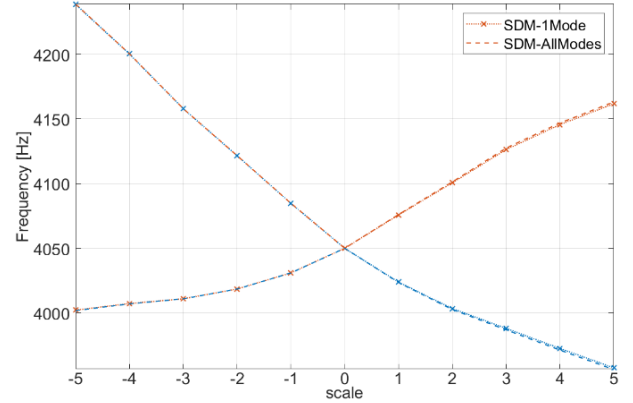


Figure 16 Absolute frequency evolution with the thickness modification

One mode is more sensitive than the other to the modification but the main focus is the relative frequency shift between the two modes

$$\frac{\Delta f(s)}{f(0)} = \frac{f_2(s) - f_1(s)}{f(0)} * 100$$

shown in Figure 17. Using positive or negative scale is almost equivalent even if frequency shift is a bit higher with negative scale (second mode frequency gets lower than the first mode frequency).

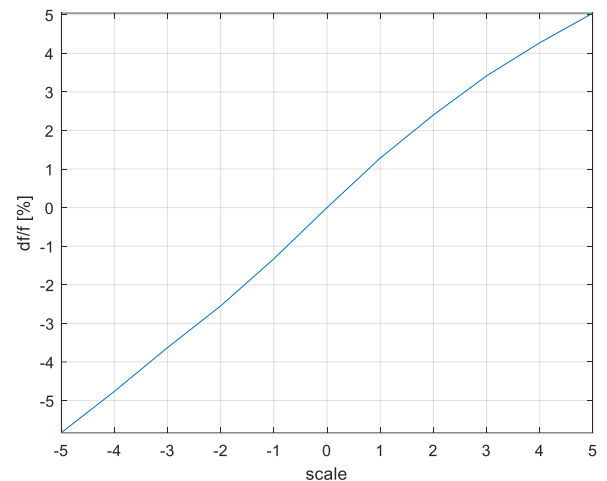


Figure 17 Relative frequency shift evolution with the thickness modification

If a frequency shift higher than 3% is for instance required, the chosen scale is -3 and the corresponding thickness modification map is shown in Figure 18.



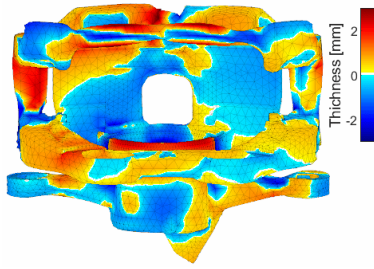


Figure 18 Final thickness distribution map to reach 3% of frequency shift

## 6. CONCLUSION

This study defines a new strategy to propose surface thickness modifications with the objective to shift frequencies associated with shapes measured during squeal occurrences. From ODS, it has been shown that a fine tuning of MDRE algorithm leads to shape estimates at all model DOFs with physically representative stress distribution. A modal model is extracted from the expanded shapes and a frequency correction is applied. Thickness sensitivity maps, computed for each mode with SDM technique, help determining areas where material addition/removal has a strong influence on the modal frequencies. A final thickness distribution map is then derived. Consistency analysis confirmed that this strategy can predict true mode shifts with accuracy. The procedure has finally been applied to an industrial brake system with the objective to separate two modal frequencies: a thickness variation map to get a 3% frequency shift has been proposed.

The proposed strategy has been developed in the Structural Dynamics Toolbox (for use with MATLAB) [19] as it provides all the necessary background for test analysis, correlation and SDM.

Using the models typically considered for CEA, one avoids the need to perform correlation and updating by considering expansion and assuming that the limit cycle frequency corresponds to modal frequencies of the expanded shapes. Thickness sensitivity maps immediately give insight to propose system modifications.

Of course, as the model is improved through correlation and update processes, the sensitivity studies should be recomputed and this is quite realistic as the computation time is not huge, typically a few hours. It is worth noting that the expansion gives information about model errors and can help updating.

The next step is obviously to test the proposed thickness modifications experimentally. Other future developments are considered:

- Optimization of thickness distribution maps from thickness sensitivity maps to respect design constraints
- Extension of the SDM strategy after MDRE to other modifications such as chamfers, local remeshing, ...
- Evaluate the robustness of stress field estimation in expanded shapes to model error and sensor location
- Instead of using ODS, try to identify modes of the brake system in operating conditions close to instability but still stable. This would give access to the root cause of the squeal; damping could be introduced (not available with ODS) and more

confidence would be gained because of a higher knowledge of the system dynamics in the modal model.

## REFERENCES

- [1] G. Martin, E. Balmes, G. Vermot Des Roches, and T. Chancelier, "Squeal measurement with 3D Scanning Laser Doppler Vibrometer: handling of the time varying system behavior and analysis improvement using FEM expansion," Sep. 2018.
- [2] G. Vermot Des Roches, O. Chiello, E. Balmes, and X. Lorang, "Squeal complex eigenvalue analysis, advanced damping models and error control," presented at the Eurobrake, May 2015.
- [3] R. J. Allemang, "The modal assurance criterion—twenty years of use and abuse," *Sound and vibration*, vol. 37, no. 8, pp. 14–23, 2003.
- [4] F. Renaud, G. Chevallier, J.-L. Dion, and G. Taudière, "Motion capture of a pad measured with accelerometers during squeal noise in a real brake system," *Mechanical Systems and Signal Processing*, vol. 33, pp. 155–166, 2012.
- [5] G. Vermot des Roches, "Frequency and time simulation of squeal instabilities. Application to the design of industrial automotive brakes.," Ecole Centrale Paris, 2011.
- [6] G. Martin, E. Balmes, and T. Chancelier, "Improved Modal Assurance Criterion using a quantification of identification errors per mode/sensor," presented at the ISMA, Leuven, Sep. 2014.
- [7] R. Jr. Craig, "A Review of Time-Domain and Frequency Domain Component Mode Synthesis Methods," *Int. J. Anal. and Exp. Modal Analysis*, vol. 2, no. 2, pp. 59–72, 1987.
- [8] R. L. Kidder, "Reduction of Structural Frequency Equations," *AIAA Journal*, vol. 11, no. 6, 1973.
- [9] A. Chouaki, P. Ladevèze, and L. Proslier, "Updating Structural Dynamic Models with Emphasis on the Damping Properties," *AIAA Journal*, vol. 36, no. 6, pp. 1094–1099, Jun. 1998.
- [10] E. Balmes, "Review and Evaluation of Shape Expansion Methods," *IMAC*, pp. 555–561, 2000.
- [11] G. Martin, G. VERMOT DES ROCHES, E. Balmes, and T. Chancelier, "MDRE: an efficient expansion tool to perform model updating from squeal measurements," 2019.
- [12] G. Martin, E. Balmes, G. Vermot Des Roches, and T. Chancelier, "Squeal measurement using operational deflection shape. Quality assessment and analysis improvement using FEM expansion.," presented at the Eurobrake, 2017.
- [13] P. Avitabile, "Twenty years of structural dynamic modification—a review," *Sound and Vibration*, vol. 37, no. 1, pp. 14–27, 2003.
- [14] A. Sestieri, "Structural dynamic modification," *Sadhana*, vol. 25, pp. 247–259, Apr. 2012, doi: 10.1007/BF02703543.
- [15] M. Corus, E. Balmes, and O. Nicolas, "Using model reduction and data expansion techniques to improve SDM," *MSSP*, vol. 20, pp. 1067–1089, 2006, doi: 10.1016/j.ymssp.2005.02.012.
- [16] W. Hunter, "Predominantly solid-void three-dimensional topology optimisation using open source software," PhD Thesis, Stellenbosch: University of Stellenbosch, 2009.
- [17] E. Balmes, "Efficient Sensitivity Analysis Based on Finite Element Model Reduction," *International Modal Analysis Conference*, pp. 1168–1174, 1998.
- [18] T. França de Paula, G. Rejdych, T. Chancelier, G. Vermot des Roches, and E. Balmes, "On the influence of geometry updating on modal correlation of brake components.,"
- [19] *Structural Dynamics Toolbox (for use with MATLAB)*. Paris: SDTools, 1995. [Online]. Available: <http://www.sdtools.com/help/sdt.pdf>

## ACKNOWLEDGEMENT

The main authors would like to thank all partners from Hitachi Astemo France for their support providing experimental data and nominal model. Their feedback throughout the whole project was greatly appreciated.